Surface-charge-governed electrolyte transport in carbon nanotubes*

Xue Jian-Ming(薛建明)[a)b)†], Guo Peng(郭 鹏)[a)], and Sheng Qian(盛 倩)[a)]

[a)] State Key Laboratory of Nuclear Physics and Technology, School of Physics, Peking University, Beijing 100871, China
[b)] CAPT, HEDPS, and IFSA Collaborative Innovation Center of MoE, Peking University, Beijing 100871, China

(Received 10 December 2014; revised manuscript received 11 March 2015; published online 20 June 2015)

The transport behavior of pressure-driven aqueous electrolyte solution through charged carbon nanotubes (CNTs) is studied by using molecular dynamics simulations. The results reveal that the presence of charges around the nanotube can remarkably reduce the flow velocity as well as the slip length of the aqueous solution, and the decreasing of magnitude depends on the number of surface charges and distribution. With 1-M KCl solution inside the carbon nanotube, the slip length decreases from 110 nm to only 14 nm when the number of surface charges increases from 0 to 12 e. This phenomenon is attributed to the increase of the solid–liquid friction force due to the electrostatic interaction between the charges and the electrolyte particles, which can impede the transports of water molecules and electrolyte ions. With the simulation results, we estimate the energy conversion efficiency of nanofluidic battery based on CNTs, and find that the highest efficiency is only around 30% but not 60% as expected in previous work.

Keywords: efficiency, surface charge, slip

PACS: 66.10.–x, 82.65.+r, 83.50.Lh, 66.10.cd **DOI:** 10.1088/1674-1056/24/8/086601

1. Introduction

Carbon nanotubes (CNTs) gain more and more attention in the development of advanced nanofluidic devices due to their unique physical properties in solution transportation.[1–6] In recent years, both simulations[7–9] and experiments[10] have indicated that the pressure-driven flow rate of water in CNTs can be several orders faster than what the continuum hydrodynamic theories predicts with a fixed boundary situation. To explain this phenomenon, slip boundary is proposed when aqueous solution flows through CNTs, which means that liquid molecules rapidly slide against the solid wall and a nonzero velocity appears at the fluid–solid interfaces in CNTs. Usually the term of "slip length" is used to characterize the magnitude of slip and it can be determined with $V_{\rm w} = b \times \partial V/\partial r$, where $V_{\rm w}$ is the velocity at the wall, b is the slip length, and r is the radius. Up to now, the slip length of water inside CNTs has been reported in a range from several nanometers to hundreds of nanometers, which depends on the system parameters, such as the diameters of CNTs.[11,12] The slip mechanism inside CNTs mainly includes the tight hydrogen-bonding network of water molecules inside CNTs,[7] and the "smoothness" of CNT wall.[13] It has been reported based on molecular dynamics (MD) simulations that the water structures in CNTs, such as the OH bond orientation and the number of hydrogen bonds in the depletion region, also contribute to the large flow rates in CNTs.[9]

CNTs with charges have many potential applications, such as bio-molecular separation and seawater desalination.[14,15] Recently, surface-charged CNT is proposed to be one of the most promising candidates to fabricate high efficient nanofluidic batteries, which can convert the hydrostatic energy into electrical power.[16] The energy conversion efficiency of a nanofluidic battery could be greatly improved with a slip channel.[16–18] In general, the energy conversion efficiencies of silica or polymer nanochannels are much less than 10%,[17–19] but with CNTs the efficiency can increase to 74% or even higher due to the large slip length of CNTs.[16] However, the above estimations are based on the assumption that the slip characteristic of charged CNTs is similar to that of uncharged CNTs. Though large slip lengths have been observed with uncharged CNTs,[10] the slip lengths in CNTs with charges have not been systematically investigated. Some studies have shown that the surface charges can influence the transport behavior of aqueous solution through CNTs under the electric field,[20–23] and also the behavior of electrolyte solution depends on nanotube diameter, salt concentration, and ion specificity.[24,25] In particular, very recently reported result indicates that surface charge can influence the ion diffusion property inside a nanopore.[26] All these results give a hint that surface-charged CNTs could have different slip lengths from the uncharged ones, therefore it is not reasonable to use the slip length found in neutral CNTs to estimate the performance of charged CNTs in their potential applications, e.g. nanofluidic battery as mentioned above. It is necessary to investigate the water transport behavior through surface-charged CNTs.

In the present work, the electrolyte transport behavior through surface-charged single-walled carbon nanotubes (SWCNT) is investigated by using MD simulations. The in-

*Project supported by the National Natural Science Foundation of China (Grant Nos. 11375031 and 11335003).
†Corresponding author. E-mail: jmxue@pku.edu.cn
© 2015 Chinese Physical Society and IOP Publishing Ltd

fluences of charge number and their spatial distribution on the transport velocity as well as on the slip length are explored. At the end of this paper, the effect of the surface charge on the energy conversion efficiency is also discussed, which can provide a useful guideline to the design of high-efficiency nanofluidic batteries.

2. Simulation methods

The simulated system is schematically illustrated in Fig. 1. The sample is composed of three parts: a single-walled carbon nanotube (SWCNT), point charges, and KCl aqueous electrolyte. The SWCNT used in the simulation has a length of 7.87 nm and a diameter of 2.17 nm. Periodic boundary condition is applied in the axial direction (along z axis). Point charges are located outside the CNT wall with a distance of 2.4 nm to the CNT center and with an evenly angular distribution as shown in Figs. 1(a) and 1(b). This is because experimentally the charges are usually produced chemically by decorating ionized molecules to the outside of CNT wall, and the excellent conductivity of CNT does not permit charges to exist in several atoms of CNT itself. In the following, "charged CNT" means a neutral CNT together with point charges, and "surface charges" means the point charges outside the tube wall. In the simulation, only the electric potential between these point charges and other particles are considered. The total charges vary from 0 e to 12 e, in steps of 3 e. In our simulations, carbon atoms and point charges are treated as rigid particles. The electrolyte solution is selected as 1-M KCl solution and a water density of 1 g/cm^3 is used. In order to keep the whole system neutral, the concentration of Cl^- is fixed at 1 M, while the number of K^+ is equal to the sum of Cl^- and point charges.

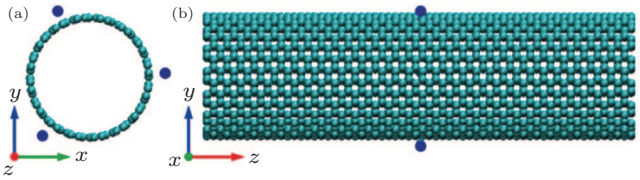


Fig. 1. (color online) Illustration of surface-charged CNTs used in the simulations in (a) top view, and (b) side view. In the figure, a (16,16) CNT is displayed and a ring including three charges is located in the middle of the tube. Water molecules and ions are not shown here. The particles outside the tube represent the negative surface charges.

Simulations are performed with LAMMPS package with the Verlet integrator.[27] TIP3P model is employed to describe water molecules,[28] K^+ and Cl^- ions are treated as charged Lennard-Jones (LJ) atoms. The interactions between carbon atoms and electrolyte particles are described by a 12-6 LJ potential, and the C–H interactions are neglected.[7] All these interactions can be described with the following equation:

$$\Phi_{mn} = 3\varepsilon_{mn}\left[\left(\frac{\sigma_{mn}}{r_{mn}}\right)^{12} - \left(\frac{\sigma_{mn}}{r_{mn}}\right)^{6}\right] + \frac{q_m q_n}{4\pi\varepsilon_0 r_{mn}}, \quad (1)$$

where r_{mn} is the distance between atom m and atom n, q_m and q_n are the charges of atom m and atom n respectively, and ε and σ are constants. Details of these potential parameters for different particles are shown in Table 1. The LJ cross parameters of wall-particles interactions were calculated with Lorentz–Berthelot rule. Details of these potential parameters could be also found elsewhere.[7,28,29]

Table 1. Potential parameters used in the MD simulation for all the particles, including the electrolyte ions of K^+ and Cl^-, water molecule, and the nanopore wall atom. The O–H distance is 0.09572 nm, and the H–O–H angle is 104.52°.

Particles	q/e	ε/(kcal/mol)	σ/nm
K^+	+1	62.74	0.325
Cl^-	–1	62.74	0.3785
O	–0.830	0.102	0.3188
H	+0.415	0	0
C–O (wall)		0.143	0.32751
Charges	–1	0	0

A cutoff radius of 1.07 nm is used in calculating LJ potentials, and the long-range Coulombic forces are computed using the particle–particle–particle–mesh solver (PPPM). Time step used in the simulation is always 1 fs, the temperature of the system is maintained at 300 K by using the Berendsen thermostat method. Non-equilibrium molecular dynamics (NEMD) simulations are carried out to obtain flow velocities and slip lengths in different situations. It is reported that the slip length obtained with equilibrium molecular dynamics (EMD) is significantly different from that obtained with NEMD.[30] In order to obtain results that are closer to the experimental situation, NEMD simulations are performed.

The system ran first in ambient conditions for 2 ns, then an external pressure is applied by a constant force along the axial direction and the system ran another 1 ns$\sim$2 ns to reach equilibrium. The force is applied only to the particles in a region of 3.0 nm $< z <$ 3.4 nm, where z is the atomic coordinate along the tube axial direction (the left end of tube is at $z = 0$). The resulting external pressure is calculated as follows: $P = f_{\text{total}}/(\pi \times R^2)$, where f_{total} is the total force applied to the atoms and R is the nanotube radius (1.085 nm). In this study, an external pressure of 10 MPa is used for all the simulations.

After the system acquires a steady velocity under the external pressure, another 2-ns simulation is performed to collect enough simulation data. The velocity profile along the radial direction is obtained by averaging these simulation data. The slip length is determined from the Navier–Stokes (NS) equation with a slip boundary:[11,16]

$$v(r) = \frac{P}{4\eta L}((R+b)^2 - r^2), \quad (2)$$

where P is the pressure difference exerted on the nanotube, $v(r)$ is the velocity at the point with distance r to the tube center, L is the tube length, R is the nanotube radius, η is the

viscosity ($\eta = 1.007 \times 10^{-3}$ Pa·s), and b is the slip length. Though the NS equation cannot accurately describe the flow behavior inside such a small nanotube, it has been shown to predict velocities in correct order of magnitude in the nanotubes with a radius higher than 0.6 nm.[31] Moreover, we focus on the relative changes with/without charges, but not on the absolute value of the slip length. Therefore we use Eq. (2) to calculate the slip length of electrolyte solution in CNTs.

3. Results and discussion

3.1. The electrolyte transport behaviors for different systems

In order to study the charge effect on the transport behaviors of electrolytes through different CNTs, we perform MD simulations on five systems: (i) pure water through uncharged CNT; (ii) 1-M KCl solution through uncharged CNT; (iii) 1-M KCl solution through CNT with three point charges and three extra K^+ ions in solution; (iv) pure water through CNT with three charges and three K^+ ions; (v) pure water through CNT with three surface charges and three extra positive charges which are located outside the CNT. In these systems, the three extra K^+ ions or three positive charges are only used to keep the system neutral. In these systems, systems (i) and (ii) has neutral CNTs, and the other three systems each have three point charges (3 e) outside the CNT wall.

The velocity profiles of these five systems are shown in Fig. 2. As seen from Fig. 2, several phenomena can be observed: i) the flow velocities at the tube wall are obviously higher than zero, which indicates the presence of the slip boundary in all these systems; ii) the velocity profiles are almost flat in all these five systems, which means that each of them has a large slip length; iii) no difference is observed in transport velocity profile between system (i) and system (ii), which indicates that adding 1-M KCl into water does not significantly influence the transport behavior through uncharged CNTs; (iv) the nearly overlapped velocity profiles for systems (iv) and (v) indicate that the presence of the three extra positive charges, which are used to balance the surface charges, does not affect the transport velocity. These results indicate that with or without surface charges (3 e), slip happens in all these five systems, but the slip length decreases significantly with presenting the three negative charges outside the CNTs.

The most important conclusion from Fig. 2 is that the transport velocities significantly decrease for all the systems with point charges ((iii), (iv), and (v)). Even when the pure water molecules transport through surface-charged CNT (e.g., systems (v) and (iv)), the flow velocity drops down from 75 m/s to 60 m/s. For 1-M KCl electrolyte solution (system (iii)), the flow velocity decreases to the lowest value of 50 m/s. With Eq. (2), a large slip length of $\sim$ 110 nm is obtained for the uncharged CNT systems (e.g., systems (i) and (ii)). This large value is consistent with the reported results in which the slip lengths range from several tens to hundreds of nanometers[9,11,32] When the three point charges are present, the slip length decreases to $\sim$ 88 nm for systems (iv) and (v), and to $\sim$ 73 nm for system (iii), respectively.

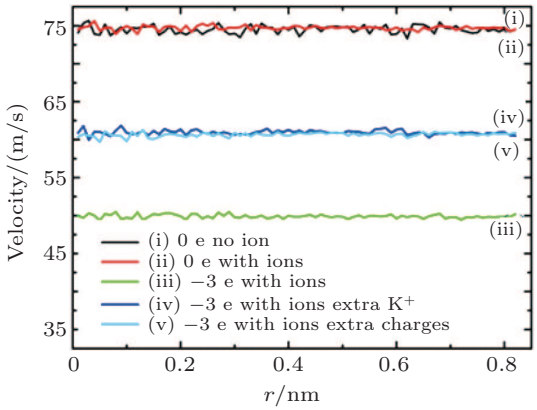


Fig. 2. (color online) Axial velocity profiles along the radial direction for the five different systems. Panels (i)–(v) represent the systems with the same letters mentioned above (see text for details). The presence of surface charge leads to the decrease of transport velocity.

The above results indicate that the transports of both water molecules and electrolyte ions through CNT can be impeded by point charges, thus the transport velocities in charged tubes are smaller than those in uncharged ones. With the three negative charges, several tens of K^+/Cl^- ions result in reducing the flow velocity from 60 m/s (system (iv)) to 50 m/s (system (iii)), and this reduction is comparable to that from 75 m/s (system (i)) to 60 m/s (system (v)) caused by nearly a thousand water molecules. This result indicates that the impeding effect contributed from per electrolyte ion is much greater than that from per water molecule.

The slip length of liquid in CNTs is dependent mainly on the friction force acting on the wall, and the large slip length of water molecules through a CNT is because of its "smooth surface", which means that the friction force at the CNT wall is very weak. For the uncharged CNTs, the friction force comes from the van der Waals attractions between the wall atoms and the liquid molecules, and it can be simplified by the C–O interactions for water molecules. When water molecules transport through the solid wall, the C–O distance can be less than the equilibrium distance and the resulting repulsive force is the source for the friction between the liquid and the solid walls.

For the charged CNTs, besides the van der Waals repulsive force, the Coulombic force between the point charges (negative) and ions (e.g. $O^-/H^+/Cl^-/K^+$) can also contribute to the solid–liquid friction force. To further explore the mechanism of the electrolyte transport through surface-charged CNTs, we analytically calculate the Coulomb potential profiles generated by the point charges along the flow direction, and the results are displayed in Fig. 3(a). The potentials on

both ends of the tube are both set to be zero. There is a potential barrier inside the charged CNTs, which would create a strong Coulombic force. When the charged particles (e.g., ions) transport through the tube, they need to overcome this potential barrier, and correspondingly the transportation of the electrolyte would be dragged down.

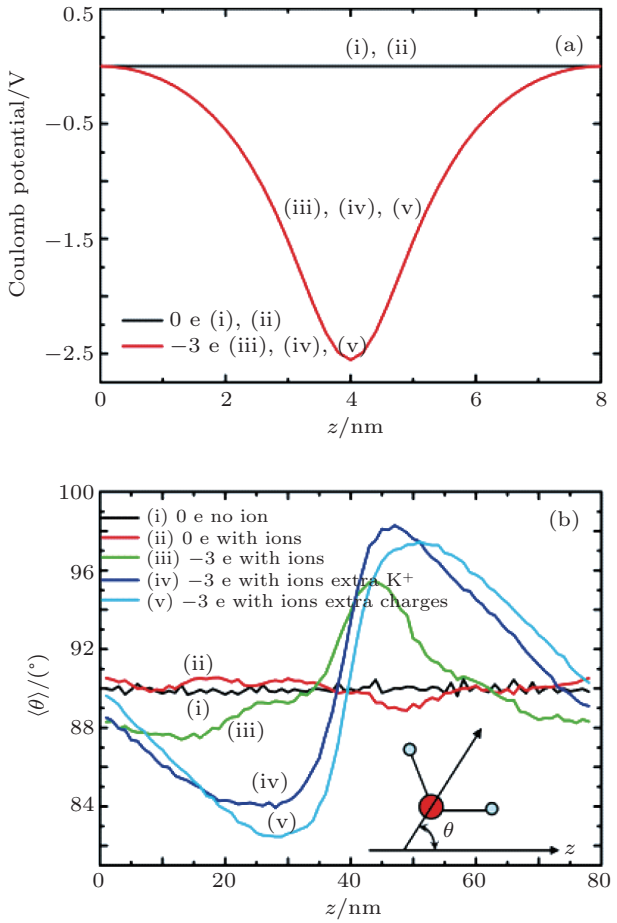


Fig. 3. (color online) (a) Coulomb potentials for surface charges of 0 e (systems (i) and (ii); black line) and −3 e (systems (iii), (iv), (v); red line). The potentials on both ends of the CNT are set to be zero. (b) Average dipole orientation distributions of water molecules along the tube axis. θ is the angle between the dipole orientation and z axis shown in insert. The average dipole orientations remain constant at about 900 in the tube without surface charge, while it fluctuates along z axis for surface-charged CNTs.

Though electric forces acting on the positive and negative ions by the negetive surface charges are opposite, all the charged particles in the solution go through accelerating and decelerating processes, and the interaction force between the solution particles and atoms of CNT (including the point charges) will be increased, resulting in increasing the friction force and reducing the flow velocity. Due to its long-distance characteristic, the Coulombic force even can significantly impede the charged particles to have a long distance from these surface charges. Because one water molecule as a whole is neutral, the contribution to the friction force from a water molecule is much less than that from an ion (Cl^-/K^+). As a result, the system with electrolytes has a larger friction force than pure water system. By taking both the van der Waals force and Coulombic force into calculation, the solid–liquid friction force follows the order from high to low among these five systems above: system (iii) > systems (iv), (v) > systems (i) and (ii), and this results in the liquid transport velocity following the same trend as displayed in Fig. 2.

Moreover, to investigate the influence of the conformation of water molecules on the water transport in CNTs, we calculate the average dipole orientation distribution of water along the z direction, which is described as the angle (θ) between a water dipole and the z axis, and the results are shown in Fig. 3(b). Without surface charges, $\langle\theta\rangle$ is always around 90° (systems (i) and (ii)), which means that there is no rotation of water molecules during their transport through CNT; while for CNTs with three surface charges, $\langle\theta\rangle$ deviation is in a range from about 83° to 98°, which indicates that the surface charges can rotate the water molecules. Due to the Coulombic interactions induced by surface charges, the water molecules near the middle of tube ($z = 40$ nm) have the largest rotation. Compared with the ordinary water molecules, rotated water systems will have more energy dissipated into the thermal energy and thus the fluid flow rate decreases. However, figure 3(b) also shows that the rotation angles of water molecules in systems (iv) and (v) are much larger (about 15°, from 83° to 98°) than that in system (iii) (∼ 8°, from 88° to 96°). Considering the fact that the flow rate of system (iii) is slower than that of system (iv)/(v) as shown in Fig. 2, this might hint that the rotation of water molecules has a weaker influence on the flow rate than that caused by the solid–liquid interaction.

3.2. Influence of the number of surface charges on the electrolyte transport behavior

In the above simulations, the surface charge is always 3 e. In experiments, the surface charge density could be different, which depends on the nanopore material and the pH value of the electrolyte solution. In this Subsection, we examine the influence of surface charge number (surface charge density) on the water transport behavior in CNTs. Other parameters are the same as those of system (iii) , only the charge number varies from 0 to 12 e. The velocity profiles and the slip length each as a function of the surface charge number are shown in Fig. 4.

The simulation results show that when the surface charge number increases from to 0 to 9 e, the transport velocity decreases quickly from 75 m/s to 10 m/s and the corresponding slip length decreases from 110 nm to 14 nm. This can be explained as follows: more surface charges generate a higher potential barrier/well inside the CNTs as shown in Fig. 4(c). As

a result, there will be a larger friction force between the solution and the CNT, and the transport velocity as well as the slip length decreases with increasing the surface charge number from 3 e to 12 e. When the surface charge number increases from 9 e to 12 e, there is no obvious difference in the transport velocity, which means that the above effect is saturated.

In most of the practical applications, a higher surface charge density is desirable. Anyhow, according to our results, increasing the surface charge density also means a lower slip length in CNTs. This effect should receive attention in optimizing systems performance by adjusting the surface charge density.

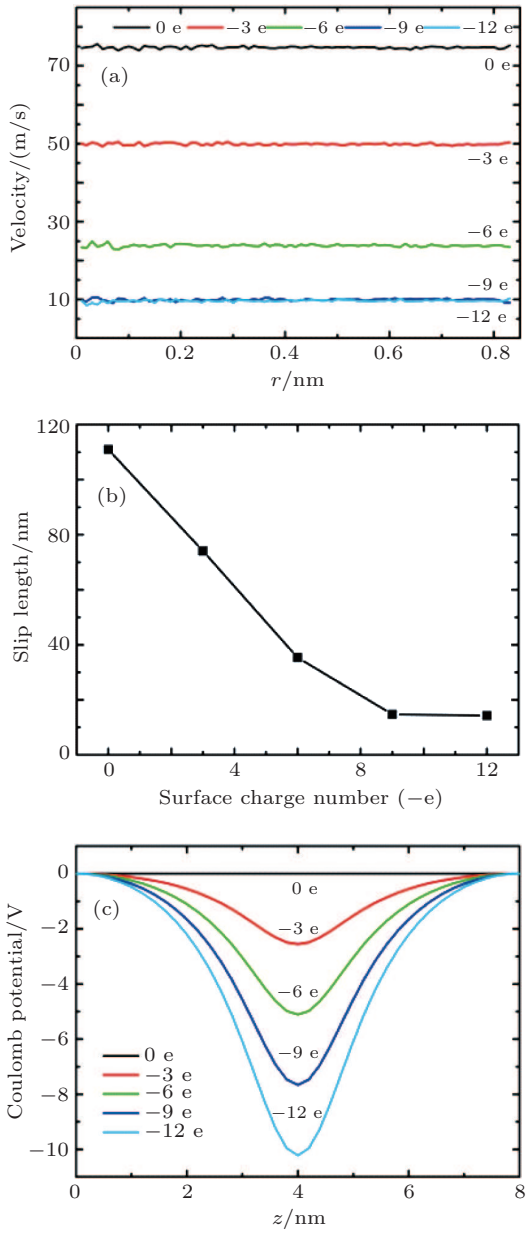


Fig. 4. (color online) Transport behaviors with the surface charge ranging from 0 e to −12 e. (a) Axial velocity profiles with different surface charge numbers. (b) Slip length as a function of the surface charge number. Slip length decreases with increasing surface charge number. (c) Corresponding Coulomb potential profiles with different surface charge numbers. A higher surface charge number generates a higher potential barrier that is more difficult for water molecules and ions to get through.

3.3. Influence of surface charge distribution pattern on the electrolyte transport behavior

In the above simulations, the surface charges are always located in one plane in the middle of the CNT. We perform the simulations for different distributions of 12 e charges around the CNTs, other parameters are the same as those shown in Subsection 3.2. The 12 e charges are averagely distributed on each of one, two and four rings out of the CNT wall. These rings are evenly separated along the CNT (see the insert of Fig. 5(b)), and the diameters of these rings are all always

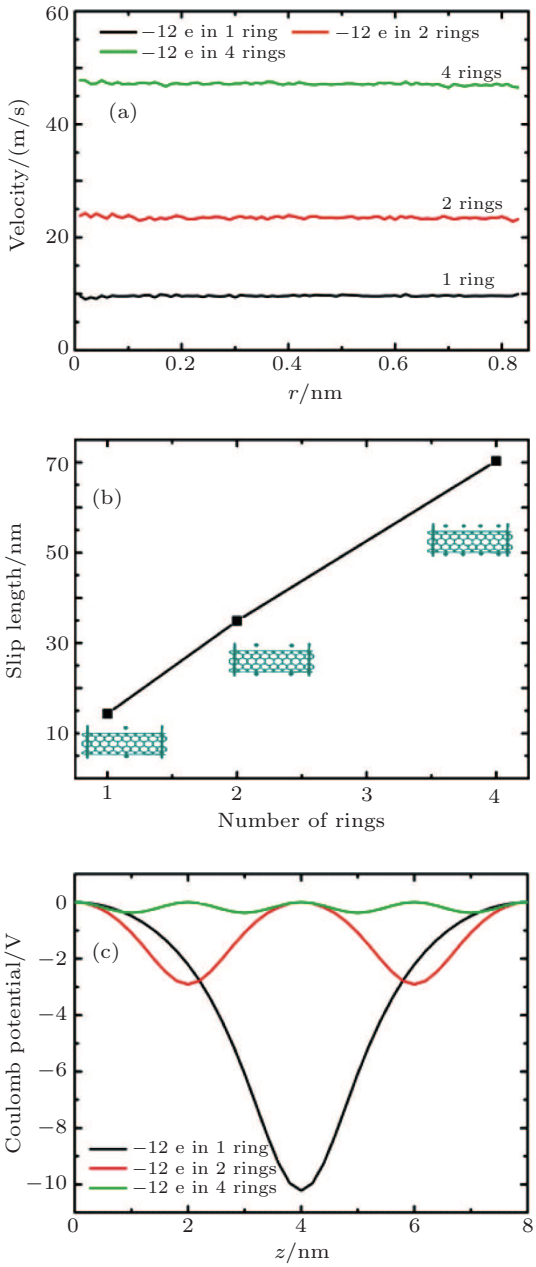


Fig. 5. (color online) Fluid transport behaviors with the different surface charge distribution patterns. The total surface charge is −12 e, with the charges distributed on 1, 2, and 4 rings, respectively. (a) Axial velocity profiles, (b) slip length as a function of the number of rings (see insets), and (c) corresponding Coulomb potential profiles for different surface charge distribution patterns. Homogenized surface charges generate a smoother electric field, which is easier for water molecules and ions to get through.

2.4 nm. As seen from Fig. 5, both the transport velocity and the slip length increase with reducing the charge number in one ring, but they are not sensitive to the number of rings along the flow direction. This phenomenon can also be explained by the Coulomb potentials along the flow direction for different surface charge distribution patterns as shown in Fig. 5(c). The number of potential wells increases with increasing the number of rings along the flow direction. However, since the total number of charges is the same for all the cases, the height of potential barrier decreases with increasing the number of rings. As discussed above, more charges along the circumference would have a stronger Coulombic interaction. For more rings along the flow direction, the surface potential becomes smoother. This smoother surface leads to a faster velocity and a larger slip length. Our simulation results reveal that the homogenization of the surface charge distribution smoothes the electric potential field along the flow direction and reduces the height of energy barrier, and as a result, the effect of surface charges becomes weaker.

The above results indicate that the slip length of the electrolyte solution transport through surface-charged CNTs is smaller than that through uncharged ones. The number of surface charges and distribution patterns will also affect the transport behavior.

3.4. Dependence of maximum energy conversion efficiency on slip length

In the following section we estimate the dependence of the maximum energy conversion efficiency ($\varepsilon_{\max}$) on the slip length obtained in our simulation. The $\varepsilon_{\max}$ is calculated based on the nonlinear Poisson–Boltzmann description of the electric double layer and the Navier–Stokes description of fluid dynamics, and the details of the method can be found in previous studies.[16–19]

Figure 6 shows the values of energy conversion efficiency ($\varepsilon_{\max}$) estimated with the slip lengths obtained in the MD simulations (shown in Fig. 4(b)). The values of $\varepsilon_{\max}$ calculated by neglecting the influence of the surface charge number on the slip length and keeping the slip length at a constant value of 110 nm are also given in Fig. 6 for comparison. The surface charge number varies from 0 to 12 e, corresponding to an effective charge density varying from 0 to -0.22 e/nm^2. As seen from the figure, the circles represent the values of $\varepsilon_{\max}$ calculated from the constant slip length value of 110 nm, and $\varepsilon_{\max}$ increases with increasing the effective surface charge density. On the other hand, the squares represent the values of $\varepsilon_{\max}$ calculated from the simulated values of the slip length. For the same value of the effective surface charge density, the value of $\varepsilon_{\max}$ is lower for the reduced slip length, and the difference between the value of $\varepsilon_{\max}$ calculated based on the constant slip length value of 110 nm and the one based on the simulated slip length value increases with increasing the effective surface charge density, i.e., the difference in the value of $\varepsilon_{\max}$ increases with increasing the difference in slip length. These results reveal that the $\varepsilon_{\max}$ would decrease significantly if the effect of surface charges on the liquid transport is taken into consideration, which indicates that the high $\varepsilon_{\max}$ predicted based on the slip length of uncharged CNTs is questionable. With the slip length values of the surface-charged CNTs obtained in our MD simulations, the $\varepsilon_{\max}$ can reach a highest value of 28%, which is still much higher than the maximum theoretical value of 7% for no-slip channels.[33] Hence, surface-charged CNTs still could be one of the most promising materials for fabricating nanofluidic battery systems.

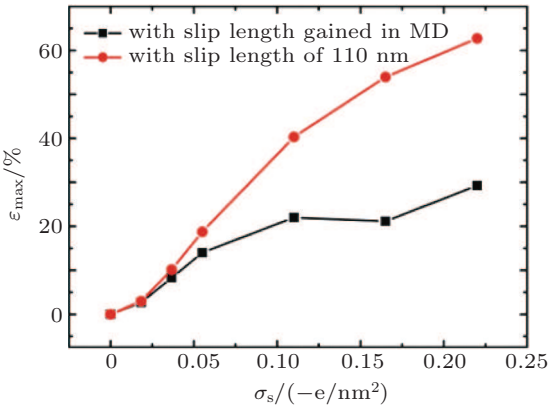


Fig. 6. (color online) Dependences of maximum energy conversion efficiency ($\varepsilon_{\max}$) of the surface-charged CNT on effective surface charge density. The nanotube used in the nanofluidic battery has a radius of 1.085 nm, and 1-M KCl is used here as the electrolyte. The number of surface charges varies from 0 to 12 e. The efficiency calculated with the slip length of the surface-charged CNT (shown in Fig. 4(b)) is much lower than that predicted with the slip length of the uncharged ones (about 110 nm), based on our MD simulations.

In experiments, the surface charge density is usually in a range of 0.01 e/nm^2–0.1 e/nm^2 for silicon-based or organic membranes,[34,35] which is comparable to what we used here. According to our simulation results, the effect of surface charge on the slip length cannot be neglected when the material is used to build nanochannels in which the slip boundary is desired. In order to obtain a large slip length, charged surfaces should be avoided, or at least the surface charges should be uniformly distributed to reduce the potential barriers.

4. Conclusions

In this work, we study the electrolyte solution transport behavior through surface-charged CNTs. The slip boundaries are observed for all charged and uncharged CNTs, but the slip lengths in charged CNTs are much smaller than those in uncharged ones. The slip length depends on the electrolyte con-

centration, the surface charge number and its distribution patterns. Our investigations demonstrate that compared with the scenario in the uncharged CNTs, the electrostatic interaction between surface charges and both electrolyte ions and water molecules in surface-charged CNTs leads to a stronger solid–liquid shearing stress, and eventually results in a lower slip length.

References

[1] Whitby M and Quirk N 2007 *Nat. Nanotech.* **2** 87
[2] Regan B C, Aloni S, Ritchie R O, Dahmen U and Zettl A 2004 *Nature* **428** 924
[3] Holt J, Park H, Wang Y, Stadermann M, Artyukhin A, Grigoropoulos C, Noy N and Bakajin O 2006 *Science* **312** 1034
[4] Bourlon B, Wong J, Miko C, Forro L and Bockrath M 2007 *Nat. Nanotech.* **2** 104
[5] Besteman K, Lee J O, Wiertz F G M, Heering H A and Dekker C 2003 *Nano Lett.* **3** 727
[6] Ghosh S, Sood A K and Kumar N 2003 *Science* **299** 1042
[7] Hummer G, Rasaiah J and Noworyta 2001 *Nature* **414** 188
[8] Kalra A, Garde S and Hummer G 2003 *Proc. Natl. Acad. Sci. USA* **100** 10175
[9] Joseph S and Aluru N R 2008 *Nano Lett.* **8** 452
[10] Majumder M, Chopra N, Andrews R and Hinds B 2005 *Nature* **438** 44
[11] Falk K, Sedlmeier F, Joly L, Netz R and Bocquet L 2010 *Nano Lett.* **10** 4067
[12] Thomas J A and McGaughey A J H 2008 *Nano Lett.* **8** 2788
[13] Sokhan V P, Nicholson D and Quirke N 2002 *J. Chem. Phys.* **117** 8531
[14] Elimelech M and Phillip W A 2011 *Science* **333** 712
[15] Shannon M A, Bohn P W, Elimelech M, Georgiadis J G, Marinas B J and Mayes A M 2008 *Nature* **452** 301
[16] Ren Y and Stein D 2008 *Nanotechnology* **19** 195707
[17] Van der Heyden F H J, Bonthuis D, Stein D, Meyer C and Dekker C 2006 *Nano Lett.* **6** 2232
[18] Xie Y B, Wang X W, Xue J M, Jin K, Chen L and Wang Y G 2008 *Appl. Phys. Lett.* **38** 163116
[19] Yan Y, Sheng Q, Wang C M, Xue J M and Chang H C 2013 *J. Phys. Chem. C* **117** 8050
[20] Li J, Gong X, Lu H, Li D, Fang F and Zhou R 2007 *Proc. Natl. Acad. Sci. USA* **104** 3687
[21] Joseph S, Mashl RJ, Jakobsson E and Aluru N R 2003 *Nano Lett.* **3** 1399
[22] Liu L, Qiao Y and Chen X 2008 *Appl. Phys. Lett.* **92** 101927
[23] Goldsmith J and Martens C C 2010 *J. Phys. Chem. Lett.* **1** 528
[24] Titus A B 2010 *J. Chem. Phys.* **132** 164513
[25] Titus A B 2011 *J. Chem. Phys.* **135** 044516
[26] Zhou X, Wang C, Wu F, Feng M, Li J, Lu H and Zhou R 2013 *J. Chem. Phys.* **138** 204710
[27] Plimpton S 1995 *J. Comp. Phys.* **117** 1
[28] Jorgensen W L, Chandrasekhar J, Madura J D, Impey R W and Klein M 1983 *J. Chem. Phys.* **79** 926
[29] Xue J M, Zou X Q, Xie Y B and Wang YG 2009 *J. Phys. D: Appl. Phys.* **42** 105308
[30] Kannam S K, Todd B D, Hansen J S and Daivis P J 2012 *J. Chem. Phys.* **136** 024705
[31] Goldsmith J and Martens C C 2009 *Phys. Chem. Chem. Phys.* **11** 528
[32] Thomas J A and McGaughey A J H 2008 *Nano Lett.* **8** 2788
[33] Daiguji H, Oka Y, Adachi T and Shirono K 2006 *Electrochem. Commun.* **8** 1796
[34] Stein, D, Kruithof M and Dekker C 2004 *Phys. Rev. Lett.* **93** 035901
[35] Xue J M, Xie Y B, Yan Y, Jin K and Wang Y G 2009 *BioMicroFluidic.* **6** 1729